

Synthesis and characterization of Pd/TiO₂ thin films with possible applications in photocatalysis

TIRADO-GUERRA, Salvador*† and VALENZUELA-ZAPATA, Miguel

Received July 18, 2017; Accepted November 25, 2017

Abstract

Synthesize thin Pd/TiO₂ films on soda-lime glass substrates, using the sol-gel chemical route and repeated immersion. Salt at 0.2 M Ti (IV) oxy acetylacetonate is dissolved in 2-methoxyethanol and stabilized with monoethanolamine, solution that is aged to obtain TiO₂ films sintered at 250 °C in air and thermal treated at 400 °C. They are surface modified with layers of palladium from a solution, following the procedure and thus the Pd/TiO₂ films. The physical and chemical properties of the prepared films are studied. The Pd/TiO₂ films are characterized in structure (XRD), morphology (SEM), chemical composition by EDS, topography (AFM), optical properties (UV-Vis) and surface analysis by XPS. Film thicknesses of 172.8 nm, a crystallite size of the order of 20 nm, transmittance of 85%, refractive indexes between 2.046-1.599, a semiconductor bandwidth of 3.67-3.50 eV, depending on the layers of palladium, resulted. The photocatalytic properties thereof were recorded, when evaluating the degradation of an aqueous test solution, as a function of the concentration and time of UV-A irradiation. The photoluminescent properties of the films were evaluated when excited with 325 nm photons. They could be applied in the treatment of water, and in radiation dosimetry.

TiO₂, sol-gel, Thin Film, Photocatalysis, Photoluminescence, Palladium

Citation: TIRADO-GUERRA, Salvador and VALENZUELA-ZAPATA, Miguel. Synthesis and characterization of Pd/TiO₂ thin films with possible applications in photocatalysis. ECORFAN Journal-Ecuador. 2017, 4-7:15-25

*Correspondence to Autor (E-mail: tirado@esfm.ipn.mx)

† Researcher contributing as first author.

Introduction

Air pollution and wastewater produced in the textile industry or in the field where technically sophisticated fertilizers, pesticides and/or detergents are used, it is quite a problem to be solved. The degradation of polluting compounds can be achieved with reactions where redox processes occur. Solar radiation can cause reactions in wide variety of organic compounds but in a limited way, as high energy (>3.3 eV) are required. Photosynthesis is a phenomenon that can remove harmful organic compounds using photo-catalysts as oxides such as TiO_2 , ZnO or SnO_2 , which are also used in catalysis (Malagutti, A.R., et al., (2009), Nejand, B.A., et al., (2010), Xin, B., et al., (2008)).

They can be simple or complex as TiO_2/WO_3 which was used to degrade rhodamine B or methyl orange (Ge, M., et al., (2009)), or composites such as ZnO/TiO_2 (Liu, G., et al., (2009)a, Ge, M., et al., (2009)) and $\text{Cu}_2\text{O}/\text{T-ZnOw}$ (Liu, G., et al., (2009)b). The degrading efficiency of a catalyst is tested with a tracer substance, based on the evaluation of the degree of degradation and mineralization to H_2O or a clean or treatable product, which is usually carried out with UV-Vis spectroscopy (Hou, J.R., et al., (2007), Ge, M., et al., (2009)).

A semiconductor such as TiO_2 or similar systems can be excited with UV radiation and from the absorbed photons, charge carriers are generated as e^- and h^+ , where the electron is ejected from the valence band VB leaving a hole, and transferred to the conduction band CB, generating electron-hole pairs (Nejand, B.A., et al., (2010)). The pairs produced can participate in reactions that decompose contaminating molecules found in the environment. Catalytic semiconductor response to UV irradiation depends on various factors: the catalyst structure, radiation, the preparation method, etc. (Xin, B., et al., (2008), Nejand, B.A., et al., (2010), Malagutti, A.R., et al., (2009)).

The photocatalytic efficiency of the semiconductor thin films (TiO_2 , ZnO) commonly improved by doping with metallic or non-metallic ions (Xin, B., et al., (2008), Chen, H., et al., (2016)) and/or deposit of precious metals (Cu, Ag, Pd), which generate levels-energy between the VB and CB bands, as vacancies, among others, which improve the optical and electrical properties, as well as photocatalytic and photoluminescence (Chae, Y.K., et al., (2013), Liu, H., et al., (2013), Dinh, C.T., et al., (2011), Malagutti, A.R., et al., (2009), Li, Q., et al., (2009), Liu, B., et al., (2014), Liu, J., et al., (2016), Wang, F., et al., (2015)).

Preparing of thin $\text{Ag}:\text{TiO}_2$ films by the polymeric precursor method, Malagutti, et al. (Malagutti, A.R., et al., (2009)) makes applications in photodegradation of textile dyes, while Dinh et al. (Dinh, C.T., et al., (2011)) using photodeposition growing techniques, colloidal clusters of Ag on TiO_2 nanocrystals which are applied in photodegradation of methylene blue and rhodamine B (Liu, F., et al., (2016)).

In this work, the synthesis of semiconductors in Pd/TiO_2 thin film prepared by the sol-gel chemical route (Brinker C.J. (1990)) and the dip coating method, as well as the study, are described. For this purpose, a series of TiO_2 films of the same thickness and then the series of Pd/TiO_2 surface modified films were prepared with several palladium deposits, the films were sintered in air at 250°C and thermally treated at 400°C . Thin films were characterized by XRD, EDS, surface properties by SEM and AFM, and their optical properties by UV-Vis. The Ti, O and Pd ionization states were determined by XPS, which is reported in the study. The effect of both, palladium deposits and conditions of preparation, on the photocatalytic properties of the films in the degradation of an aqueous solution of methyl orange (MO) at 14 ppm, and also which are the effects on their emission spectra, when samples are irradiated with UV (325 nm), evaluated.

From such study, determine the possible of application of Pd/TiO₂ films, in homogeneous photocatalysis and in radiation dosimetry, to mention this two cases. Since the thin-film TiO₂ semiconductor has a bandwidth of the order of 3.2 eV, it is known that it can be modified, in fact reduced, when the film is doped with metals of Au, Ag, Cu, among others, or is superficially modified with similar materials, such as Pd. Thus, using the method of the chemical route and repeated immersion, technique already implemented, Pd/TiO₂ films from appropriate precursors will be synthesized, varying the palladium deposits and at a temperature of 250 °C and a thermal treatment at 400 °C.

It is desired to study the effect on the structural, morphological and optical properties of the films, as well as the photocatalytic properties when irradiating with UV-Vis and degrading a tracer substance, and the photoluminescence presented by the Pd/TiO₂ series of films when they are irradiated with UV.

The order of presentation is, introduction and justification, methodology experimental, synthesis, characterization techniques, results and discussion are given by technique: XRD, SEM and EDS, AFM, UV-Vis and XPS, photodegradation and photoluminescence, conclusions, acknowledgments and references.

Methodology experimental

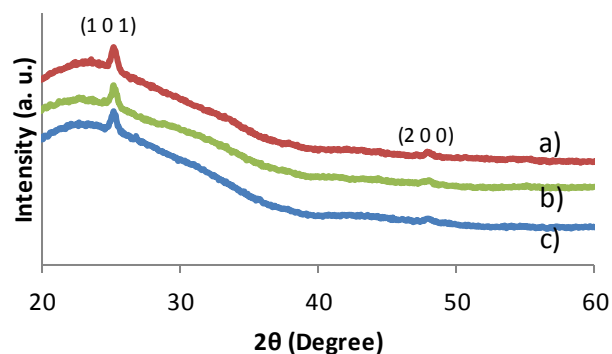
Synthesis

Series of Pd/TiO₂ films were prepared by the sol-gel route, and dip coating technique, from a solution (100 mL) of titanium oxy-acetylacetonate (IV) salt (TiO(C₅H₇O₂)₂) at 0.2 M in 2-methoxyethanol (C₃H₈O₂) as solvent, and monoethanolamine ((C₂H₅O)NH₂) as stabilizer at 23 °C, for 2 h with constant magnetic stirring, and an aqueous solution of palladium nitrate dihydrate (N₂O₆Pd•2H₂O) at low concentration. The solution was aged for seven days before being used in the growth of films. The samples resulted with an average thickness of 172.8 nm.

X-ray diffraction

Diffraction patterns were recorded on a PANalytical X'Pert PRO MRD diffractometer model, with Cu tube K_α (λ = 0.15406 nm) at 45 kV voltage and 40 mA of tube current, using the Bragg-Brentano geometry, θ-2θ, the spectra were recorded in the range of 15-80° with a step of 0.03° and time of 200 s accounts with an aperture of 0.5°. XRD diffractograms of the Pd/TiO₂ films were polycrystalline with diffraction peaks at 25.281, 36.947 and 48.050° to name a few, and they correspond to the (1 0 1), (1 0 3) and (2 0 0) planes, respectively (see graphic 1).

These drawings were indexed according to 021-1272 card of TiO₂ anatase phase (tetragonal, space group 141/amd with cell parameters: a = b = 3.7852 Å and c = 9.5139 Å at 90° angles, the known Scherrer's formula, $D = 0.9 \lambda / \beta \cos \theta$, with λ wavelength of Cu K_α (λ = 0.15406 nm), θ is angular peak position and β is the semi-width of the peak given in radians, was used to estimate the crystallite size, and resulted a D ~ 20 nm.



Graphic 1 Diffraction patterns of Pd/TiO₂ films, (a) for pure sample, (b) with one layer of palladium and (c) samples with three layers of palladium.

Scanning electron microscopy

SEM micrographs of Pd/TiO₂ films were recorded on a QUANTA 3D FEG SEM microscope (FEI) and representative x10000 magnification micrographs are shown in Fig. 2a) and 2b).

The micrograph of the Pd/TiO₂ pure films (Fig. 1a)) has an uneven and porous morphology, however for micrograph in Fig. 1b) of the Pd/TiO₂ films with a surface deposited with Pd can be observed a morphology more uniform with fine grains and growth in areas (lights) corresponding to nanoparticles of Pd, with EDS analysis the presence of palladium nanoparticles was detected, the surface distribution of the growth of the nanoparticles was uniform, making more evident the surface distribution and increased grain size (image not shown).

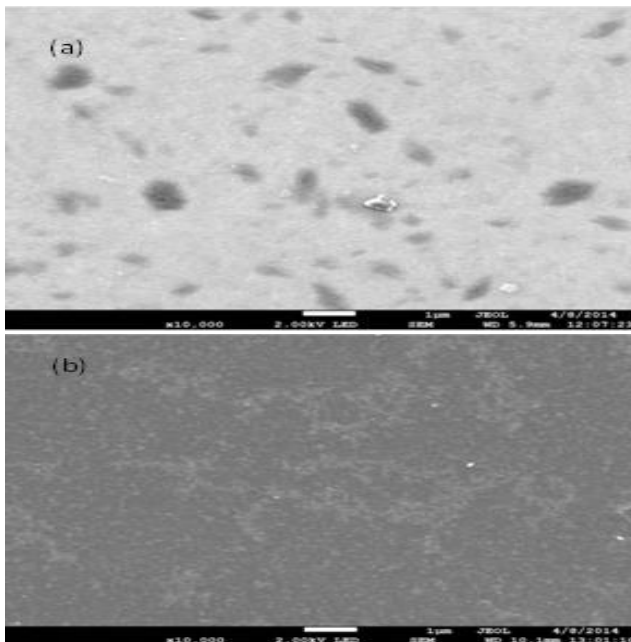


Figure 1a) and 1b) SEM micrographs increased x10000, (a) Pd/TiO₂ pure and (b) Pd/TiO₂ samples with one layer of palladium

Atomic force microscopy

Topographical and morphological characteristics of Pd/TiO₂ films were recorded on a Park AutoProbe CP Equipment, atomic force microscope (Veeco) with a tip of silicon 10 microns, intermittently. 3D topographical (AFM) representative images of Pd/TiO₂ pure and modified films with a layer of palladium are shown in Fig. 2a) and 2b), respectively. It is observed the grain surface density in the order of 42 grains/µm².

In the 2D image of Fig. 3, the marker line and the corresponding profile, the distribution and grain sizes are shown. The average grain size is really small (around 0.1 µm or less) and roughness parameters were, Rq = 1.16 nm and Ra = 0.886 nm in a 1x1 µm².

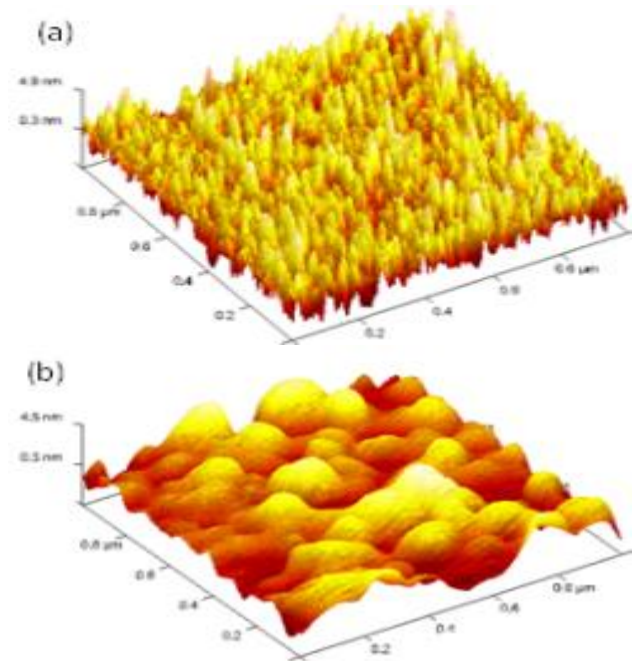


Figure 2a) and 2b) 3D images AFM, (a) Pd/TiO₂ pure and (b) Pd/TiO₂ with one palladium layer, respectively

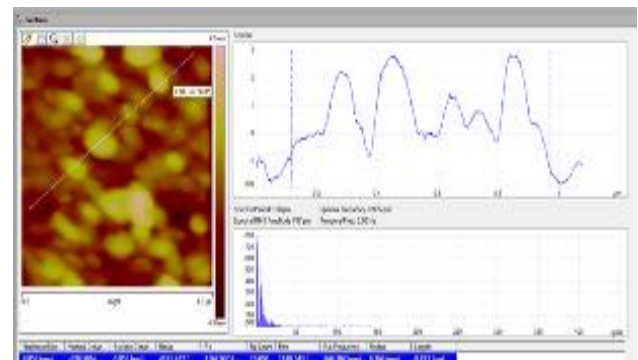
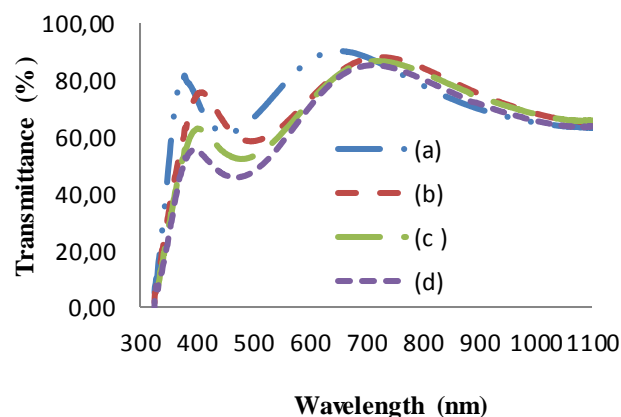


Figure 3 2D image of Pd/TiO₂ with a palladium layer and the cross-sectional profile indicated in the picture

Ultraviolet-visible spectroscopy

UV-Vis spectra of Pd/TiO₂ films (graphic. 2) were recorded on a UV-Vis Perkin Elmer model Lambda 2 spectrophotometer, a deuterium lamp (²H) was used for the UV region and a tungsten one for the visible region, the spectra were recorded in the range of 190-1100 nm in wavelength. The board absorption was recorded in 381 nm (pure) and at 417 nm for the film with a layer of Pd, while the transmittance was 85 % and 80 %, respectively. From the visible part of spectra the thickness of the films was estimated at 172.8 nm in pure films and 162.4 nm in films with a layer of Pd.

The indices of refraction were in the range of 2.046-1.599 and 2.262-1.672 for pure sample and for samples with a layer of Pd, respectively, the refractive index of samples with more catalyst deposits were in the order. Likewise, in the region of high energies of these spectra the bandwidth E_g of Pd/TiO₂ semiconductors, was evaluated, resulting 3.67, 3.62 and 3.50 eV for pure sample, and with 1 and 3 layers of palladium, respectively, it can be observed a red shift when the layers of Pd are increased, and using the fact that the TiO₂ semiconductor has an indirect band, from a graph of $(kh\nu)^{1/2} = A(h\nu - E_g)$ extrapolation to the axis of photons. A is a constant and k is related to the Kubelka-Munk constant, the E_g value was obtained (Murphy, A.B., et al., (2007), Patcharee, J., et al., (2012), Ilican, S., et al., (2008)). The relationship $\alpha(\lambda) = \ln(1/T)/d$ gives the dependence of the refractive index with wavelength λ , was used to obtain the value for d film thickness.



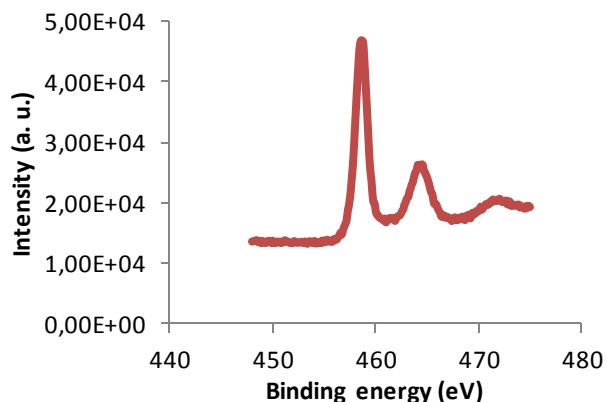
Graphic 2 UV-Vis spectra of the Pd/TiO₂ films, (a) pure film, and (b), (c) and (d) films with one, three and five layers of palladium

Spectroscopy of photoelectron

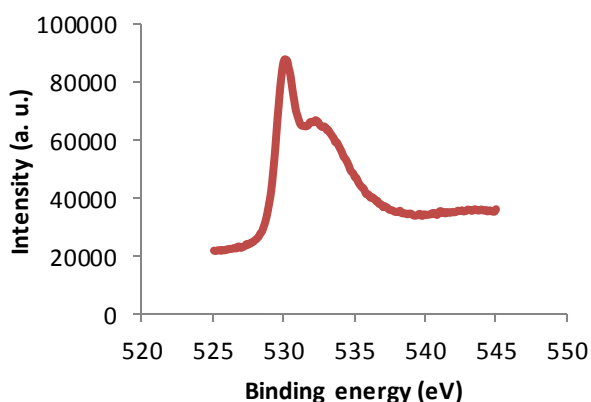
Through spectroscopy of photoelectron (XPS) (Thermo Scientific K Alfa, Double Source Mg and Al) the ionization states of Ti, O, and Pd, and the binding energies of the respective orbitals, were evaluated. Graphic 3 shows the high resolution XPS spectra for the Ti2p (graphic 3) orbital, O1s (graphic 4) orbital, and the Pd3d orbital (graphic 4), respectively. The energy of the Ti2p (2p_{3/2}, 2p_{1/2}) orbital, with maximum intensities at 458.78 and 464.58 eV, respectively, for systems of TiO₂:Cu prepared by sol-gel, Xin et al. evaluated the energy of the 2p_{3/2} level at 458.1 eV (Xin, B., et al., (2008)). For O1s, the highs in 530.28 and 533.88 eV linked to species of oxygen, e.g. oxygen of lattice and possible oxygen adsorbed, respectively (Dinh, C.T., et al., (2011), Liu, H., et al., (2013), Liu, F., et al., (2016)).

From the spectra recorded for the Pd/TiO₂ systems, the orbital energy of Pd3d (3d_{5/2}, 3d_{3/2}), the maximum values resulted around 336.88 and 342.28 eV, respectively, Brun, M., et al. reported for the 3d_{5/2} orbital, 335.4 eV (Brun, B., et al., (1999)). It is observed a sub-structure in the high resolution spectrum Pd3d (335.48 and 340.98 eV) with a $\Delta E = 5.50$ eV.

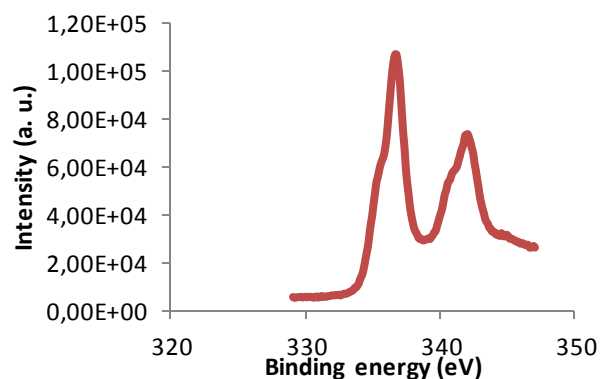
The Pd3d double peaks can show the presence of metallic Pd and PdO as reported (Hoflund, G.B., et al., (2003), Brun, B., et al., (1999)). All peaks of spectra were determined relative to the energy of the carbon C1s orbital (284.68 eV), that gives the calibration for the peaks in the spectra of Pd/TiO₂ semiconductors.



Graphic 3 High resolution XPS spectrum of the orbital Ti2p (2p_{3/2}, 2p_{1/2}) at 458.78 and 464.58 eV in binding energy, respectively.



Graphic 4 High resolution XPS spectrum of the O1s orbital with peaks at 530.28 and 533.88 eV in binding energy that can be linked to different oxygen species.



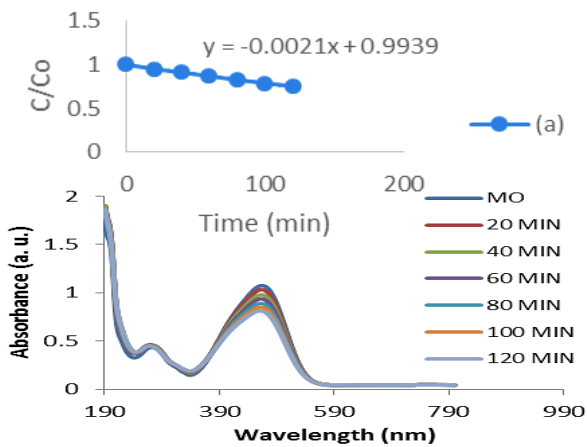
Graphic 5 Energy of Pd3d orbital (3d_{5/2}, 3d_{3/2}), the maximum values resulted around 336.88 and 342.28 eV, respectively. The Pd3d double peaks can be observed.

Photocatalytic activity

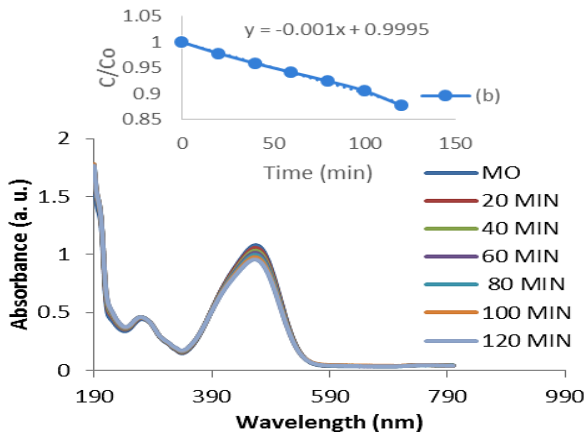
The photocatalytic properties of the Pd/TiO₂ catalysts were probed in the degradation of an aqueous solution of methyl orange to 14 ppm, irradiating the samples of 1 cm² area (two-sided) with six fluorescent lamps at different times in a photo-reactor Luzchem LCZ-5 and the photo-degradation of the solution in the 190-800 nm range, was registered in a Cintra 20 of GBC spectrophotometer, while from an integrating sphere the diffuse absorbance of the solution was evaluated, 100 mL of aqueous solution of methyl orange were prepared in volumetric flask, from which were used aliquot of 3 mL.

The procedure was to record the absorbance of the non-irradiated aliquot and from the main band at 464.0 nm, its evolution was followed when the aliquot-catalyst system, was irradiated each 10 min until completing 120 min. The behavior of a set of 4 samples (pure, and those with 1, 3 and 5 deposits of palladium) was recorded. If C₀ is the initial concentration and C the concentration of the solution for a given irradiation time, the kinetics of the reaction follows the equation $K[C] = -d[C]/dt$, and when it is integrated gives $\ln[C]/[C_0] = -k^t$, and the plot of $\ln[C]/[C_0]$ versus irradiation time, t , the slope corresponds to the pseudo reaction constant (Malagutti, A.R., et al., (2009), Liu, F., et al., (2016), Wang, F., et al., (2015)).

In order to show the catalytic activity of Pd/TiO₂ semiconductors, it is given in graphic 6 and graphic 7, the TiO₂ catalytic response of the pure systems and films with one palladium layer, spectra correspond to the non-irradiated aqueous solution and for 20, 40, 60, 80, 100 and 120 min irradiation time (each case). The insert slope in graphs shown, are related to the constant of the reaction. It is expected that systems with several palladium deposits present a greater catalytic activity than those corresponding to the pure TiO₂ system.



Graphic 6 Photodegradation of the pure TiO₂ film depending on the wavelength, and the inserted graph showing the variation of the concentration of the solution as a function of irradiation time.

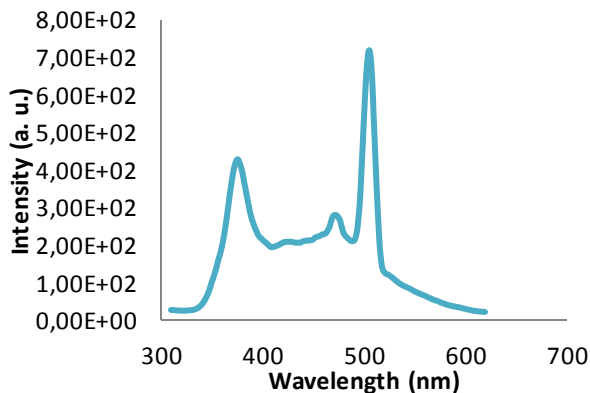


Graphic 7 Photodegradation of Pd/TiO₂ film with one palladium layer, depending on the wavelength, and the inserted graph showing the variation of the concentration of the solution as a function of irradiation time.

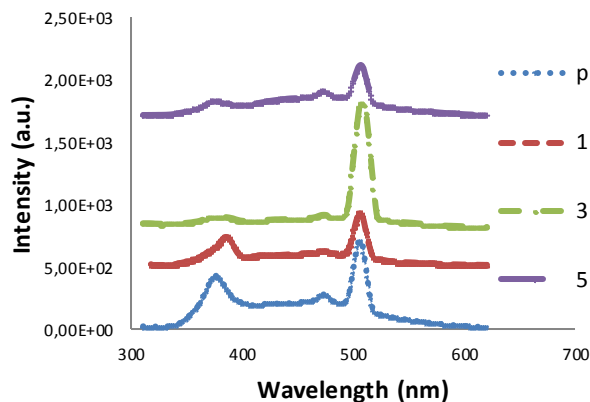
Photoluminescence

The luminescent properties of the Pd/TiO₂ films were recorded at room temperature in a Shimadzu RF-5301 spectrofluorophotometer. The excitation energy corresponds to a wavelength of 325 nm, and the corresponding emission spectra were recorded in the 310 to 620 nm range. Three major bands are defined in the photoluminescence spectra of Pd/TiO₂ films, for UV region is about 375 nm and in the visible region at 473 and 505 nm, respectively, while at 425 nm was defined a broad emission band in the pure film, while the spectrum of the film with three palladium layers is different, where a wide band of low intensity is formed of two possible bands to 370 and 385 nm, and in the visible region, two bands at 469 and 505 nm are formed, the last being the most intense. The spectrum for 520 nm presents a fading that tends to zero at 600 nm. Respective emission spectra are shown in graphics. 8 and 9.

The crystal size of the samples, from XRD was estimated at $D \sim 20$ nm, which could be related to size of the bands of the UV spectra and where the films are thin (Hirai, T., et al., (2005)), it could having the effect of the confined excitons, and therefore in the charge recombination processes. Furthermore, it is known that films prepared by the sol-gel and dipping process, containing surface states and defects and also vacancies, among others, they are active agents in the possible mechanisms that generate the photoluminescence spectra (Li, Q., et al., (2009), Gao, X., et al., (2013), Liu, G., et al., (2009)a) and so are our systems that have been prepared by the sol-gel method. The main peak in the visible (505 nm) is practically the typical peak emission whose position remains fixed, although its presence depends on the ratio of anatase-rutile phases of TiO₂.



Graphic 8 Photoluminescence spectrum of the pure Pd/TiO₂ film with four emission bands, one important in the UV region and two in the visible region



Graphic 9 Photoluminescence spectra of films, pure, one, three and five layers of palladium, Pd/TiO₂, a wide band in the UV region and two emission bands in the visible region

Results and discussion

The Pd/TiO₂ films were polycrystalline with diffraction peaks corresponding to the (1 0 1), (1 0 3) and (2 0 0) planes, respectively (see graphic. 1). The peaks were indexed according to the card no. 0021-1272 for anatase phase of TiO₂. The pure Pd/TiO₂ film provided an uneven and porous morphology, and the Pd/TiO₂ films with a surface deposit of Pd, a more uniform fine grains and growth of Pd nanoparticles (EDS analysis) morphology, were obtained.

The thin films showed a morphology with very small grains, while the average grain size was in the order of 0.1 μm or less, and roughness parameters $R_q = 1.16 \text{ nm}$ and $R_a = 0.886 \text{ nm}$ from a full $1 \times 1 \mu\text{m}^2$ image, were recorded. The films showed high transmittance, with interference effects and the bandwidth of the films showed a red shift with the number of layers of palladium catalyst, 3.67 to 3.50 eV, which means in principle, best catalytically and photoluminescent properties in films with more layers of palladium. Liu, G. et al. (Liu, G., et al., (2009)a), in composites ZnO/TiO₂ systems evaluated a $E_g = 3.84 \text{ eV}$, while Malagutti, et al. (Malagutti, A.R., et al., (2009)), with the percentage of Ag, modified the bandwidth E_g of Ag/TiO₂ systems, when they implemented the degradation of an aqueous solution of rhodamine B.

In the high resolution spectra of the Ag/TiO₂ systems, Malagutti, et al. (Malagutti, A.R., et al., (2009)) sets for the orbital O1s two peaks, that of 530.0 eV was associated with the Ti-O bond, while the small peak was associated with the link Ti-OH (with maximum at 532.0 eV), in our case was 530.28 eV for the main peak and possible lattice oxygen, slightly higher value, representing a somewhat different chemical environment. The signal at 533.88 eV could be associated with a group of surface carbon (Dinh, C.T., et al., (2011)) or possible oxygen adsorbed on TiO₂ surface (Liu, H., et al., (2013)). The high resolution of Pd3d spectrum shows signals associated to metallic Pd and PdO (Hotflund, G.B., et al., (2003), Brun, B., et al., (1999)).

From the graph of C/C_0 versus irradiation time (insets in graphic 6 and 7), the slope is related to the pseudo reaction constant (Malagutti, A.R., et al., (2009)), which happens to be a reaction of first order with respect to the C concentration. Fig. 7a) shows the properties of catalytic activity of Pd/TiO₂ semiconductors, for the system without palladium and film with one layer of palladium (graphic 7).

For 0, 20, 40, 60, 80, 100 and 120 min irradiation times, thus the photocatalytic property of thin Pd/TiO₂ films, whose efficiency should be improved with surface modifications with Pd, as had being reported improvements in systems such as Ag:TiO₂ (Malagutti, A.R., et al., (2009), Dinh, C.T., et al., (2011)), among others.

Films prepared are thin and the estimated crystal sizes, could be having the effect of confined excitons and therefore in the recombination processes of e⁻ and h⁺ (Hirai, T., et al., (2005)). Furthermore, it is known that films prepared by the sol-gel and dipping process, containing surface states and defects and also vacancies, among others, which are active agents in the possible mechanisms that generate the photoluminescence spectra (Li, Q., et al., (2009), Gao, X., et al., (2013)).

Conclusions

The semiconductor Pd/TiO₂ thin film is grown on soda-lime substrates using the sol-gel process and repetitive dives. The films have the crystal structure of the anatase phase of TiO₂, with a porous morphology in pure and pore-free and uniform in those deposited with palladium, with grain growth uniformly distributed over the surface of the films, the topography of the sample shows grains rounded of various sizes, but especially in very thin films, the roughness was in the order of 1.0 nm and a surface density of 42 grains/μm² was assessed, films had good optical properties with high transmittance and especially their properties of catalytic activity in the degradation of methyl orange in particular the TiO₂ system, and the corresponding to the film with one layer of Pd, with a poor catalytic response than the pure sample, the response of the samples with three and five palladium layers, was not so different.

The experimental results of the photoluminescent properties of the TiO₂ films having both emission bands in the UV and in the visible region with the well-defined band at 505 nm, which is enhanced in one order of magnitude in Pd/TiO₂ films, in particular with three deposits of palladium, relative to the pure film. In films with one and five Pd deposits, the bands in the UV attenuate their presence and the intensity of the band in the visible is diminished, especially in the film with five layers of palladium.

Factors that influence the properties of films, both catalytic and photoluminescent, are the conditions of synthesis, morphology and porosity, film thickness, concentration of the co-catalyst, atmosphere of growth in the synthesis, and especially the treatment temperature to achieve greater crystallinity of the films. Partial results presented show significant potential applications in both degradation of substances polluting water and air, as well as applications in their photoluminescent properties of these films of titanium dioxide, and surface modifications with metal as Pd, Ag, between others.

Acknowledgments

SIP-IPN Research Projects 20141245 and 20171063, to Natzin Tirado for editing this paper and to Ing. Omar Rios Berny by recording the photodegradation and photoluminescence spectra.

References

- Brinker C. J., (1990). Sol-gel science: the physics and chemistry of sol-gel processing, Oval Road, London: Academic Press Limited.
- Brun B., Berthet A. & Bertolini J.C., (1999). XPS, AES and Auger parameter of Pd and PdO. Journal of Electron Spectroscopy and Related Phenomena, 104, 55-60.

- Chae Y.K., Park J.W., Mori S. & Suzuki M., (2013). Photocatalytic effects of plasma-heated TiO_{2-x} particles under visible light irradiation. *Korean J. Chem. Eng.*, 30 (1), 62-66.
- Chen H., Tang M., Rui Z., Wang X. & Ji H., (2016). ZnO modified TiO₂ nanotube array Pt catalyst for HCHO. *Catalysis Today*, 264, 23-30.
- Dinh C.T., Nguyen T.D., Kleitz F. & Do T-On., (2011). A new route to size and population control of silver clusters on colloidal TiO₂ nanocrystals. *Applied Materials and Interfaces*, 2228-2234.
- Gao X., Chen J. & Yuan C., (2013). Enhancing the performance of free-standing TiO₂ nanotube arrays based dye-sensitized solar cells via ultraprecise control of the nanotube wall thickness. *J. Power Sources*, 503-509.
- Ge M., Guo C., Zhu X., Ma L., Han Z., Hu W. & Wang Y., (2009). Photocatalytic degradation of methyl orange using Zn/TiO₂ composites. *Front Environ. Sci. Eng. China* 3 (3), 271-280.
- Hirai T., Harada Y., Hashimoto S., Itoh T. & Ohno N., (2005). Luminiscence of excitons in mesoscopic ZnO particles. *J. Lumin.* 112, 196-199.
- Hoflund G.B., Hoglin H.A.E., Weaver J.F. & Salaita G.N., (2003). ELS and XPS study of Pd/PdO methane oxidation catalysis. *Applied Surface Science* 205, 102-112.
- Hou J.R., Yuan C.Z. & Yang P., (2007). Nanotube composites with photocatalytic activity for degradation of ethylene blue under UV irradiation. *J. Hazard. Mate. B*, 310-315.
- Ilican S., Caglar Y. & Caglar M., (2008). Preparation and characterization of ZnO thin films deposited by sol-gel spin coating method. *Journal of Optoelectronics and Advanced Materials* 10 (10), 2578-2583.
- Keun Chae Y., Won Park J., Mori Shinsuke & Masaaki Suzuki Masaaki, (2013). Photocatalytic effects of plasma-heated TiO_{2-x} particles under visible light irradiation. *Korean J. Chem. Eng.*, 30(1), 62-63.
- Li Q., Chen Y., Zhang X., Su Y. & Jia C., (2009). Annealing effect on the morphologies and photoluminescence properties of ZnO nanocombs. *J. of Phys. and Chem. of Solids*, 70, 1482-1486.
- Liu B., Liu L-M., Lang X-F., Wang H-Y. & Lou X-W., (2014). Doping high-surface-area mesoporous TiO₂ microspheres with carbonate for visible light hydrogen production. *Energy & Environmental Science*, 7, 2592-2597.
- Liu F., Yan X., Chen X., Tian L. & Xia Q., (2016). Mesoporous TiO₂ nanoparticles terminated with carbonate-like groups: Amorphous/crystalline structure and visible-light photocatalytic activity. *Catalysis Today*, 264, 243-249.
- Liu G., Li G., Qiu X. & Li L., (2009)a. Synthesis of ZnO/titanate nanocomposites with highly photocatalytic activity under visible light irradiation. *Journal of Alloys and Compounds* 481, 492-497.
- Liu G., Yan X., Chen Z., Wang X., Wang L., Lu G. Q. & Cheng Hui-Ming, (2009)b. Synthesis of rutile-core-shell structured TiO₂ for photocatalysis. *J. Mats. Chemistry*, 19, 6590-6596.
- Liu H., Wang J., Fan X.M., Zhang F.Z., Liu H.R., Dai J. & Xiang F.M., (2013). Synthesis of Cu₂O/T-ZnOw nanocompound and characterization of its photocatalytic activity and stability property under UV irradiation. *Materials Science and Engineering B* 178, 158-166.

Liu J., Han L., Ma H., Tian H., Yang J., Zhang G., Seligmann B.J., Wang S. & Liu J., (2016). Template-free synthesis of carbon doped TiO₂ mesoporous microplates for enhanced visible light photodegradation. *Science Bulletin*, doi: 10.1007/s1434-016-1162-3.

Malagutti A.R., Maurá Henrique A.J.L., Garbin J.R. & Ribeiro C., (2009). Deposition of TiO₂ and Ag/TiO₂ thin films by the polymeric precursor method and their application in the photodegradation of textile dyes. *Applied Catalysis B: Environmental* 90, 205-212.

Murphy A.B., (2007). Band-gap determination from diffuse reflectance measurements of semiconductor films, and application to photoelectrochemical water-splitting. *Solar Energy and Solar Cells* 91, 1326-1337.

Nejand B.A., Sanjabi S. & Ahmadi V., (2010). The effect of sputtering gas pressure on structure and photocatalytic properties of nanostructured titanium oxide self-cleaning thin film. *Vacuum* 85, 400-405.

Patcharee J., Pongsaton A., Sumentha S. & Tanakorn R., (2012). Surface and photocatalytic properties of ZnO thin film prepared by sol-gel method. *Thin Solid Films* 520, 5561-5567.

Wang F., Li F-L., Xu M-M., Yu H., Zhang J-G., Xia H-T. & Lang J-P., (2015). Facile synthesis of a Ag(I)-doped coordination polymer with enhanced catalytic performance in the photodegradation of azo dyes in water. *J. Materials Chemistry A*, 3, 5908-5916.

Xin B., Wang P., Ding D., Liu J., Ren Z. & Fu H., (2008). Effect of Surface on Cu-TiO₂